# Low-energy exclusive cross sections and inclusive production of identified charged hadrons with Babar

J. William Gary

Department of Physics and Astronomy
University of California, Riverside, CA, 92521 USA

Recent measurements of exclusive hadronic cross sections from the Babar Collaboration at SLAC are presented. Specifically, we present results on the $e^+e^- \to K^+K^-(\gamma)$, $p\bar{p}$, $K_S K_L$, $K_S K_L \pi^+\pi^-$, $K_S K_S \pi^+\pi^-$, and $K_S K_S K^+K^-$ cross sections performed using events with initial-state photon radiation, which allows the cross sections to be measured at low energy and over an extended energy range. In addition, we present results on the inclusive momentum spectra of identified charged pions, kaons, and protons at the fixed center-of-mass energy of 10.54 GeV, allowing new tests of QCD.

## 1. Introduction

The Babar experiment operated at the PEP-II asymmetric-energy $e^+e^-$ collider at SLAC from 1999-2008. The data analysis is still very active, with around 30 physics publications expected in 2013. Most data were collected at the energy of the $\Upsilon(4S)$ resonance, just above the threshold to produce a $B\bar{B}$ bottom-quark meson pair. The $B\bar{B}$ event sample was (and still is being) used to study CP violation and to probe the physics of the Cabibbo-Kobayashi-Maskawa quark-mixing matrix. Babar also collected large samples of $e^+e^- \to c\bar{c}$ and $e^+e^- \to \tau^+\tau^-$ events and has many results on charm meson and tau lepton physics. The topics of the current presentation are something yet different, however: events with initial-state photon radiation (ISR), which give access to measurements of low-energy exclusive $e^+e^-$ cross sections, and recent results on the inclusive production of identified charged hadrons ($\pi^\pm$, $K^\pm$, p) at the fixed center-of-mass energy of 10.54 GeV.

## 2. The $e^+e^- \to K^+K^-(\gamma)$ cross section and $K^\pm$ form factor

Our recent measurement of the $e^+e^- \to K^+K^-(\gamma)$ cross section [1] fits into a broad Babar ISR program to provide a precise low-energy measurement of the inclusive $e^+e^- \to hadrons$ cross section by summing exclusive
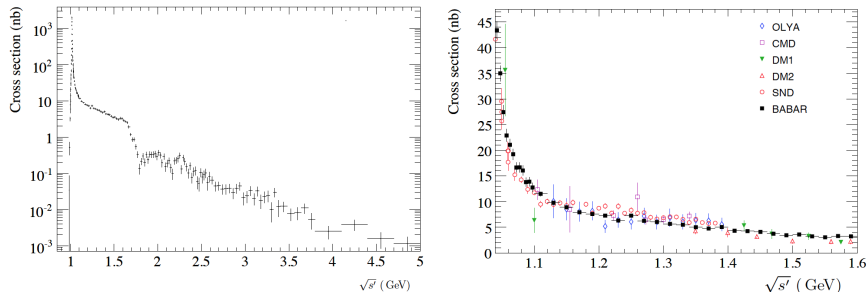
Fig. 1. Babar results for the $e^+e^- \rightarrow K^+K^-(\gamma)$ cross section, (left) over the full energy range probed and (right) in the $1.04 \leq \sqrt{s'} \leq 1.60$ GeV region.

channels. One measures the $\sigma(e^+e^- \rightarrow X \gamma_{ISR})$ cross section, with "X" the exclusive state, as a function of the mass $\sqrt{s'} = m_X$ of the state, where $\sqrt{s'}$ is the effective c.m. energy. The sum of exclusive channels provides a more accurate determination of the cross section than a measurement based on the inclusive recoil against the ISR photon $\gamma_{ISR}$ because it yields better mass ($\sqrt{s'}$) resolution. With the $K^+K^-$ results presented here, Babar covers essentially the complete set of significant exclusive channels.

The low-energy $e^+e^- \rightarrow hadrons$ inclusive cross section is needed for the calculation of the hadronic correction to the vacuum polarization contribution to the muon magnetic anomaly $a_\mu$, namely for the standard model prediction of the muon $g-2$ value. Note that $a_\mu$ cannot be calculated perturbatively. Instead one uses the measured low-energy $e^+e^- \rightarrow hadrons$ inclusive cross section in conjunction with dispersion relations.

We measure the number of $K^+K^-(\gamma)$ events in intervals of $\sqrt{s'}$. We allow the possibility of an additional photon "$(\gamma)$," beyond the ISR photon, in order to keep the uncertainty of the event acceptance below $10^{-3}$. The luminosity is monitored by measuring the number of $\mu^+\mu^-(\gamma)$ events within the same data sample. Thus knowledge of the absolute luminosity is not necessary and there is no reliance on theoretical expressions for radiator functions, reducing systematic uncertainties.

Events are required to contain two charged tracks consistent with a $K^+K^-$ pair. The photon with highest energy is identified as the ISR photon. The ISR photon must have at least 3 GeV in the c.m. frame and lie within 0.3 radians of the missing momentum vector formed from all other reconstructed particles in the event (this last requirement strongly suppresses non-ISR events). Background events, which mostly arise from other ISR processes, are subtracted, and the data are corrected to account for finite detector resolution.

The measured cross section is shown in Fig. 1 (left). The Babar results
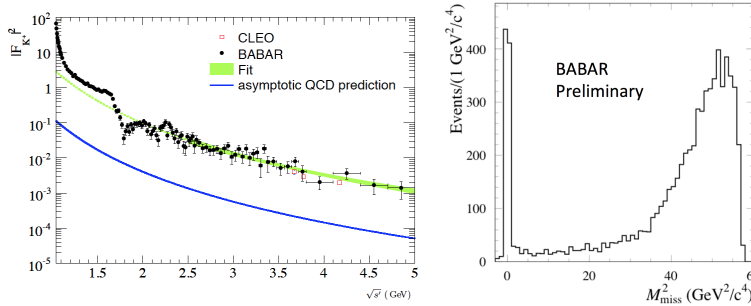
Fig. 2. (left) The charged kaon form factor measurement from Babar. The solid green line shows the result of a fit of the QCD shape $\alpha_S(s')/s'$ to the data. The solid blue line shows the QCD result including the predicted absolute normalization. (right) The missing-mass-squared distribution (preliminary) for untagged $\gamma_{ISR}$ events in the $e^+e^- \rightarrow p\overline{p}$ channel.

cover a large energy range compared with previous experiments and six orders of magnitude in cross section. The precision of the results is emphasized in Fig. 1 (right), which shows the Babar results in a zoomed energy range in comparison with results from other experiments. Concerning the muon anomaly, the Babar results yield $a_\mu^{KK,LO} = 22.93 \pm 0.18(\text{stat.}) \pm 0.22(\text{syst.})$, compared with the previous result $a_\mu^{KK,LO} = 21.63 \pm 0.27(\text{stat.}) \pm 0.68(\text{syst.})$, and thus improve the precision of the KK contribution to $a_\mu$ by about a factor of three.

We also extract the charged kaon form factor, shown in Fig. 2 (left). For $\sqrt{s'} \geq 2.5$ GeV, in the region above the hadron resonances, the shape of the QCD prediction $\alpha_S(s')/s'$ (with $\alpha_S$ the strong coupling strength) agrees with the data. However the predicted normalization is wrong by an order of magnitude. The Babar measurements agree with those from the CLEO experiment [2], shown by the three red squares in Fig. 2 (left). CLEO has results at three energy points only because they use fixed c.m. energies rather than the ISR method.

## 3. The proton form factor

A similar ISR technique to that described above for $e^+e^- \rightarrow K^+K^-(\gamma)$ events is used to select $e^+e^- \rightarrow p\overline{p}$ events. Babar has two recent studies of the $p\overline{p}\gamma_{ISR}$ channel: one where the photon is reconstructed in the detector ("tagged") [3] and one where it is not ("untagged") [4]. The tagged analysis updates a previous Babar publication [5] using twice as much data and improved analysis techniques. In the untagged analysis, which is preliminary,
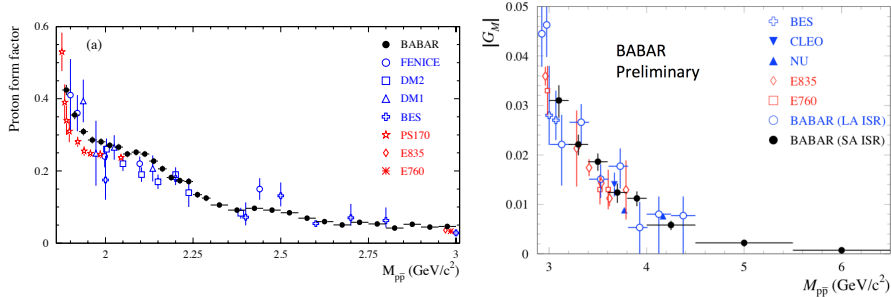
Fig. 3. The proton form factor measurement from the (left) tagged-$\gamma_{\mathrm{ISR}}$ p$\overline{\text{p}}$ analysis at low $\sqrt{s'}$ and (right) from the untagged (preliminary) and tagged analyses at high $\sqrt{s'}$, in comparison with the results from other experiments.

the ISR photon is colinear with the beam axis, leading to a p and $\overline{\text{p}}$ that can be widely separated in phase space and thus to events with a large p$\overline{\text{p}}$ invariant mass. The untagged analysis greatly improves the precision of the results for $\sqrt{s'} > 3$ GeV.

For the untagged analysis, the key selection variables are the summed transverse momentum of the identified p and $\overline{\text{p}}$ and the missing-mass-squared $M^2_{\mathrm{miss}}$ recoiling against the p$\overline{\text{p}}$ pair (both quantities should be about zero for signal events). Figure 2 (right) shows the measured $M^2_{\mathrm{miss}}$ distribution after all selection criteria for the analysis are applied except for that on $M^2_{\mathrm{miss}}$: a clear signal peak with little background is seen at $M^2_{\mathrm{miss}} \approx 0$.

Figure 3 shows our measurements of the proton form factor. The left plot, from the tagged analysis (large angle "LA" $\gamma_{\mathrm{ISR}}$), confirms the enhancement of the $e^+e^- \to$ p$\overline{\text{p}}$ cross section just above the p$\overline{\text{p}}$ threshold and demonstrates the precision of the Babar results over a wide energy range. The right plot, from the untagged analysis (small angle "SA" $\gamma_{\mathrm{ISR}}$) illustrates the much increased precision achieved at high mass values with the untagged sample.

## 4. The $e^+e^- \to K_S K_L$, $K_S K_L \pi^+ \pi^-$, $K_S K_S \pi^+ \pi^-$, and $K_S K_S K^+ K^-$ channels

These studies, currently all preliminary, are also based on the ISR technique. For the $e^+e^- \to K_S K_L$ analysis, we require events to contain exactly one $K_S \to \pi^+ \pi^-$ candidate that is consistent with arising from the primary interaction point (IP) and to have no charged tracks consistent with the IP. The $K_L$ detection efficiency is measured from data using events in the dominant $e^+e^- \to \phi\gamma_{\mathrm{ISR}} \to K_S K_L \gamma_{\mathrm{ISR}}$ channel: a clean $K_L$ signal is seen, even though no explicit $K_L$ selection criteria are applied. We then apply
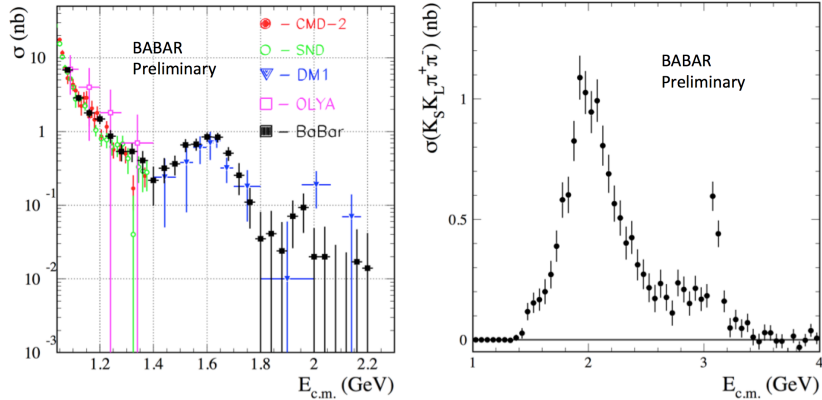
Fig. 4. Cross section measurements of the (left) $e^+e^- \to K_S K_L$ and (right) $e^+e^- \to K_S K_L \pi^+\pi^-$ processes (preliminary).

$K_L$ selection criteria to this sample, identifying a $K_L$ candidate as an isolated cluster in the electromagnetic (EM) calorimeter with energy larger than 0.2 GeV and within 0.5 radians of the expected $K_L$ direction based on the event kinematics. The $K_L$ detection efficiency is thereby measured to be around 48%, about 6% lower than predicted by the simulation. Corresponding corrections are subsequently applied to the simulated $K_L$ detection efficiency as a function of the $K_L$ energy and direction.

We then study the non-resonant $e^+e^- \to K_S K_L$ channel ($K_S K_L$ invariant mass larger than 1.06 GeV). Contributions from $e^+e^- \to K_S K_L (n\pi^0)$ events with $n \geq 1$ are suppressed by requiring the energy of additional EM clusters in the event to be less than 0.5 GeV. Sidebands in the data are used to evaluate and subtract residual background. The results for the $e^+e^- \to K_S K_L$ cross section are shown in Fig. 4 (left). The Babar data are seen to be precise and to cover a larger energy range than previous experiments, as for the $K^+K^-$ and $p\bar{p}$ analyses presented above. Clear evidence is obtained for production through the $\phi(1600)$ resonance: we observe around 1000 events in the $\phi(1600)$ region, compared to 58 events for the only previous measurement in this region, from the DM1 experiment in 1981 [6].

Similar techniques are used to study the $e^+e^- \to K_S K_L \pi^+\pi^-$, $K_S K_S \pi^+\pi^-$, and $K_S K_S K^+K^-$ channels. These are the first measurements ever for these three cross sections. As an example, the results for the $e^+e^- \to K_S K_L \pi^+\pi^-$ cross section are shown in Fig. 4 (right). A clear $J/\psi$ meson peak is observed. Clear $J/\psi$ peaks are also seen in the $K_S K_S \pi^+\pi^-$ and $K_S K_S K^+K^-$ channels. From the $J/\psi$ results, we extract the first measurements of the corresponding $J/\psi$ branching fractions, which are summarized

Table 1. $J/\psi$ branching fractions from the $e^+e^- \to K_S K_L \pi^+\pi^-$, $K_S K_S \pi^+\pi^-$, and $K_S K_S K^+ K^-$ analyses.

| Branching fraction ($\times 10^{-3}$) | Babar (preliminary) | PDG (2012) |
|---|---|---|
| $\mathcal{B}_{J/\psi \to K_S K_L \pi^+\pi^-}$ | $3.7 \pm 0.6 \pm 0.4$ | No entry |
| $\mathcal{B}_{J/\psi \to K_S K_S \pi^+\pi^-}$ | $1.68 \pm 0.16 \pm 0.08$ | No entry |
| $\mathcal{B}_{J/\psi \to K_S K_S K^+ K^-}$ | $0.42 \pm 0.08 \pm 0.02$ | No entry |

in Table 1.

## 5. Identified charged hadron production

The final topic is not about ISR events but rather about the inclusive production of identified charged pions, kaons, and protons at $E_{\text{c.m.}} = 10.54$ GeV [7], with $E_{\text{c.m.}}$ the c.m. energy. The multiplicity and momentum spectra of identified charged hadrons provide a basic characterization of multihadronic events as well as information on how hadronization depends on hadron mass, strangeness, and baryon number.

Precise measurements of identified charged hadron spectra at energies around 91 GeV were provided by the LEP and SLD experiments. However, until the present work and and roughly contemporaneous results from the Belle Collaboration [8], the only $e^+e^-$ annihilation results on identified charged hadrons at $E_{\text{c.m.}} \approx 10$ GeV were from the ARGUS experiment [9]. The BES experiment presented distributions of inclusive charged particle multiplicity and momentum for c.m. energies between around 2 and 5 GeV [10], but not results for identified hadrons.

The Babar analysis makes use of 0.91 fb$^{-1}$ of data collected in the $e^+e^-$ continuum region at 10.54 GeV. This represents only about 0.2% of the total Babar data sample but is sufficient because the uncertainties are dominated by systematic terms. Charged tracks are required to have momenta above 200 MeV so that the particle identification (PID) efficiencies are well determined. In total, 2.2 million events are selected. As for all the studies discussed above, Monte-Carlo-(MC)-simulation-derived track-selection and PID efficiencies are corrected to account for data-MC discrepancies using control samples in the data. The background, which primarily arises from $e^+e^- \to \tau^+\tau^-$ events, is subtracted. We mostly use prompt particles in presenting results, which means that the decay products of $K_S$ mesons and weakly decaying baryons are not included. This differs from the convention generally used by the LEP and SLD experiments.

The results for the inclusive identified charged hadron spectra are shown in Fig. 5 (left). The data are displayed in bins of $x_p = 2p^*/E_{\text{c.m.}}$, where $p^*$ is the c.m. particle momentum. The results are shown (from top to
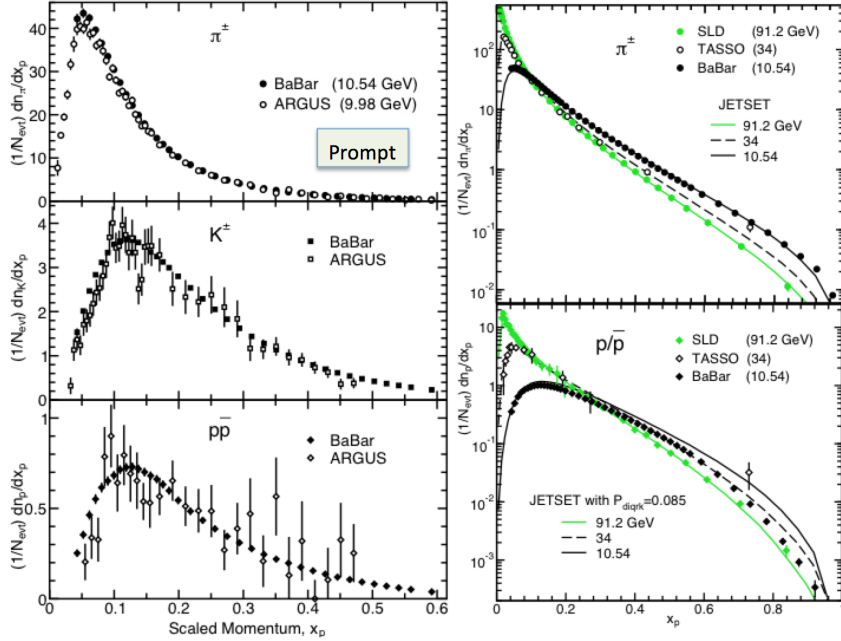
Fig. 5. (left) Scaled momentum spectra for charged pions, kaons, and protons; (right) Comparison of the scaled momentum spectra of charged pions and protons for the SLD, TASSO, and Babar experiments.

bottom) for charged pions, kaons, and protons. The corresponding results from ARGUS are also shown. The Babar and ARGUS data agree once the small difference in c.m. energy is accounted for. The Babar data for kaons and protons are seen to be far more precise than those of ARGUS.

The precise low $E_{c.m.}$ Babar data allow the scaling behavior to be investigated. Figure 5 (right) shows the Babar data (black points) for charged pions (top) and protons (bottom) in comparison with the corresponding results from SLD at 91.2 GeV [11] (green points). Intermediate-energy results from the TASSO experiment [12] are also shown. Clear scaling violations are observed, i.e., the Babar and SLD data do not agree with each other. At large values of $x_p$, the scaling violation is attributed to the running of the strong coupling strength $\alpha_S$, while at small $x_p$ it is a hadron-mass effect. Shown in comparison with the data are predictions from the Jetset [13] MC event generator. The green and black Jetset curves correspond to $E_{c.m.} = 10.54$ and 91.2 GeV, respectively. For charged pions (top right plot of Fig. 5), the black curve goes through the black points and the green curve through the green points, so the scaling behavior is well described.

For protons, however (bottom right plot of Fig. 5), the black curve lies above the black points, indicating that the scaling violation is overestimated by the simulation.

## 6. Summary

Babar has a strong and comprehensive program in the measurement of exclusive $e^+e^- \rightarrow$ *hadrons* cross sections using the ISR method. Summing the exclusive channels yields improved results for the inclusive cross section, which is important for the precision of the standard model prediction for the muon anomaly $a_\mu$. The ISR method allows precise measurements of exclusive cross sections over an extended effective c.m. energy range. Recent Babar results based on the ISR method are presented for the the $e^+e^- \rightarrow K^+K^-(\gamma)$, $p\bar{p}$, $K_SK_L$, $K_SK_L\pi^+\pi^-$, $K_SK_S\pi^+\pi^-$, and $K_SK_SK^+K^-$ processes.

In addition, precise measurements of the inclusive momentum spectra of identified charged pions, kaons, and protons at $E_{c.m.} = 10.54$ GeV are presented. These results allow new tests of QCD predictions, both for scaling violations and MLLA calculations (the comparison of data with MLLA results is omitted from this report due to length constraints).

## References

[1] J.P. Lees *et al.* (Babar Collaboration), Phys. Rev. D **88**, 032013 (2013).

[2] T.K. Pedlar *et al.* (CLEO Collaboration), Phys. Rev. Lett. **95**, 261803 (2005).

[3] J.P. Lees *et al.* (Babar Collaboration), Phys. Rev. D **87**, 092005 (2013).

[4] J.P. Lees *et al.* (Babar Collaboration), arXiv:1308.1795.

[5] B. Aubert *et al.* (Babar Collaboration), Phys. Rev. D **73**, 012005 (2006).

[6] F. Mané *et al.* (DM1 Collaboration), Phys. Lett. B **99**, 261 (1981).

[7] J.P. Lees *et al.* (Babar Collaboration), Phys. Rev. D **88**, 032011, 2013.

[8] M. Leitgab *et al.* (Belle Collaboration), Phys. Rev. Lett.**111**, 062002 (2013).

[9] H. Albrecht *et al.* (ARGUS Collaboration), Z. Phys. C **44**, 547 (1989).

[10] J.Z. Bai *et al.* (BES Collaboration), Phys. Rev. D **69**, 072002 (2004).

[11] K. Abe *et al.* (SLD Collaboration), Phys. Rev. D **59**, 052001 (1999).

[12] W. Braunschweig *et al.* (TASSO Collaboration), Z. Phys. C **42**, 189 (1989).

[13] T. Sjöstrand, Comput. Phys. Commun. **82**, 74 (1994).